HHS Public Access

Author manuscript

J Mol Cell Cardiol. Author manuscript; available in PMC 2019 January 01.

Published in final edited form as:

J Mol Cell Cardiol. 2018 January ; 114: 58–71. doi:10.1016/j.yjmcc.2017.10.004.

Regulation of Ca^{2+} signaling by acute hypoxia and acidosis in rat neonatal cardiomyocytes

José-Carlos Fernández-Morales[1] and **Martin Morad**[1,2]

[1]Cardiac Signaling Center of MUSC, USC and Clemson, Charleston, South Carolina

[2]Department of Pharmacology, Georgetown University Medical Center, Washington, DC, USA

Abstract

Ischemic heart disease is an arrhythmogenic condition, accompanied by hypoxia, acidosis, and impaired Ca^{2+} signalling. Here we report on effects of acute hypoxia and acidification in rat neonatal cardiomyocytes cultures.

Results—Two populations of neonatal cardiomyocyte were identified based on inactivation kinetics of L-type I_{Ca}: *rapidly-inactivating* I_{Ca} (τ~20ms) myocytes (prevalent in 3-4-day cultures), and *slow-inactivating* I_{Ca} ($\tau \geq 40$ms) myocytes (dominant in 7-day cultures). Acute hypoxia (pO_2 < 5 mmHg for 50–100s) suppressed I_{Ca} reversibly in both cell-types to different extent and with different kinetics. This disparity disappeared when Ba^{2+} was the channel charge carrier, or when the intracellular Ca^{2+} buffering capacity was increased by dialysis of high concentrations of EGTA and BAPTA, suggesting critical role for calcium-dependent inactivation. Suppressive effect of acute acidosis on I_{Ca} (~40%, pH 6.7), on the other hand, was not cell-type dependent. Isoproterenol enhanced I_{Ca} in both cell-types, but protected only against suppressive effects of acidosis and not hypoxia. Hypoxia and acidosis suppressed global Ca^{2+} transients by ~20%, but suppression was larger, ~35%, at the RyR2 microdomains, using GCaMP6-FKBP targeted probe. Hypoxia and acidosis also suppressed mitochondrial Ca^{2+} uptake by 40% and 10%, respectively, using mitochondrial targeted Ca^{2+} biosensor (mito-GCaMP6).

Conclusion—Our studies suggest that acute hypoxia suppresses I_{Ca} in *rapidly inactivating* cell population by a mechanism involving Ca^{2+}-dependent inactivation, while compromised mitochondrial Ca^{2+} uptake seems also to contribute to I_{Ca} suppression in *slowly inactivating* cell population. Proximity of cellular Ca^{2+} pools to sarcolemmal Ca^{2+} channels may contribute to the

Corresponding author: Prof. Martin Morad, Cardiac Signaling Center, USC, MUSC & Clemson University, Charleston, SC. 29425, Phone number: +1(843) 792-3898, Fax number: +1(843) 792-0664, moradm@musc.edu.

Competing interests

No conflicts of interest, financial or otherwise, are declared by the author(s).

Author contributions

Designed the experiments: M. Morad

Conducted experiments and analysis: JC Fernandez-Morales

Wrote the manuscript: JC Fernandez-Morales, and M. Morad

variability of inactivation kinetics of I_{Ca} in the two cell populations, while acidosis suppression of I_{Ca} appears mediated by proton-induced block of the calcium channel.

Keywords

L-type Ca(2+) channel; ischemia; hypoxia; acidosis; neonatal rat cardiomyocytes

INTRODUCTION

Cardiac L-type calcium channels are critical in maintaining the duration of cardiac action potential, initiation of pacemaker activity, triggering of contraction, and are implicated in oxygen- and mechano-sensing of the heart [1–2]. In neonatal heart, however, sarcolemmal Ca^{2+} influx and efflux appears to be more important for contraction-relaxation cycle than Ca^{2+} uptake and release by the SR [3], because of poorly developed SR with predominantly peripherally located couplons and RYRs [4–5]. With the onset of myocardial ischemia the heart becomes rapidly hypoxic and acidotic, increasing the transient outward potassium current, shortening action potentials, suppressing calcium current, compromising the calcium signaling pathways, and leading eventually to arrhythmia and heart failure [6–7], ischemic myocardium responds to hypoxia by switching to glycolytic metabolism, which in turn causes accumulation of lactic, and phosphoric acids that decrease the myocardial pH.

During birth and few days afterwards the new-born often encounters episodes of hypoxia/acidosis. Birthing events such as uterine contractions during delivery could compress the umbilical cord and reduce blood flow. Complications from shoulder dystocia, umbilical cord prolapse or retention of the head may also lead to hypoxia/acidosis episodes [8–9]. Recurrent apnoea with acute intermittent hypoxic episodes is also a major clinical problem in preterm infants, often leading to autonomic dysfunction as the augmented ventilatory response to hypoxia [10], and cardiac arrhythmias [11]. Survival potential of the new-born under hypoxic conditions appears to critically depend on appropriate release of catecholamines from chromaffin cells of adrenal medulla, regulated similarly by L-type calcium channel [12–14].

Extracellular acidification plays a critical role not only in calcium channel regulation [15], and signal transduction, but also in gating of a family of acid-sensing ion channels (ASIC) [16], which are activated in cardiac sensory neurons during an ischemic episode [17]. Intracellular acidification has been similarly implicated in cellular signal transduction, initiation of cellular proliferation and triggering of apoptosis [18]. Acute acidosis during myocardial ischemia also triggers series of changes in the electrophysiological and biochemical events that include slowing of signal conduction, suppression of Na^{+} and Ca^{2+} currents [19–20], change in myofilament Ca^{2+} sensitivity [21], and inhibition of specific intracellular biochemical pathways [22]. It has also been reported that acidosis suppresses the enhancing effects of β-adrenergic agonists on the L-type Ca^{2+} channel in guinea-pig cardiomyocytes [23], and that interleukin-1 restores the β-adrenergic sensitivity of I_{Ca} in the presence of acidosis [24].

Here we have attempted to quantify the effects of ischemia (hypoxia and/or acidosis) on the Ca^{2+} channel, Ca^{2+} signalling and mitochondrial Ca^{2+} uptake in rat neonatal cardiomyocytes

(rN-CM), which appear to express either slowly or rapidly inactivating L-types Ca^{2+} channels. The hypoxic suppressive effect on I_{Ca} was larger in slowly inactivating cells, while the acidosis effect showed no significant differential suppression on the two cell types. Hypoxia suppressive effects were larger on the Ca^{2+} μ-domains associated with RyR2 than on the global cytosolic Ca^{2+} transients, possibly related to significant suppression of mitochondrial Ca^{2+} uptake by hypoxia. These findings suggest multiplicity of mechanisms with distinct kinetics and specificity that mediate the oxygen- and pH-sensing of the L-type Ca^{2+} channels and Ca^{2+} signalling, requiring targeted Ca^{2+} probes to measure their specific effects on subcellular Ca^{2+} signalling.

METHODS

Ethical approval

Protocols for experiments with rats (AR no. 2791) was approved and supervised by the Institutional Animal Care and Use Committees (IACUC) of Georgetown University, the Medical University of South Carolina (A 3428–01), University of South Carolina (A 3049-01) and the Department of Veterans Affairs according to national and international guidelines. All efforts were made to minimize animal suffering.

Culture of neonatal rat cardiomyocytes

Four- to six-day-old neonatal rats were decapitated, the chest cavities opened, hearts excised, and the main vessels and atria removed. The ventricles were minced with a razor blade and incubated in Hank's Balanced Salt Solution (HBSS, Invitrogen) with trypsin (50 μg/ml) for 14–16 h at 4 °C [25]. The digestion was then arrested by exposure to trypsin inhibitor (200 μg/ml) for 20 min. Collagenase (100 U/ml) was used for 30 min to isolate single rN-CM, which were then filtered and centrifuged at 1000 rpm for 3 min, re-suspended in Dulbecco's Modified Eagle's Medium (DMEM) containing 10% fetal bovine serum (FBS) with 1% penicillin–streptomycin and 1% non-essential amino acids, plated on 100-mm dishes and placed in the incubator for 60 min to eliminate fibroblasts rN-CM overall viability was ~80%. Isolated single rN-CM were plated onto non-treated glass 25-mm cover slips and used for electrophysiological experiments.

Electrophysiological recordings

For patch-clamp recording of whole-cell Ca^{2+} currents (I_{Ca}) the perforated-patch mode of the patch-clamp technique was used [26–27], using amphotericin B (1mg/ml) as the permeating agent [28–29]. Tight seals (>1 GΩ) were achieved with the intracellular solution that had the following composition (in mM): 145 Glutamic Acid, 9 NaCl, 1 $MgCl_2$ and 10 HEPES, pH 7.2~7.3, adjust with CsOH. The standard extracellular Tyrode's solution used contained (in mM): 137 NaCl, 1 $MgCl_2$, 2 or 5 $CaCl_2$, 2 or 5 $BaCl_2$ (depending on the experimental protocol), 5.3 KCl, 10 glucose, and 10 HEPES. The duration of each different experimental treatment (Normoxia/Hypoxia and/or pH 7.4/pH 6.7, with or without ISO, 2Ca/2Ba (Normoxia/Hypoxia or pH 7.4/pH 6.7), 5Ca (pH 7.4)/5Ca (pH 6.7)) in all the figures of the manuscript was always 100s, excepts for the experiments with nifedipine, where the wash/out was extended for 2–3 minutes, with nickel where the steady-state was

reached in 30 seconds or the experiments with different holding potential (−40/−60 mVs), where the protocol was extended only by 15 s.

I_{Ca} was recorded at room temperature (22–25 °C) using a Dagan voltage-clamp amplifier controlled by pClamp-9 software running on a personal computer. Borosilicate patch pipettes with 5–8 MΩ resistance were prepared using a horizontal pipette puller (Model P-87, Sutter Instruments, CA). The series resistance was monitored until it decreased to < 30 MΩ, the liquid junction potential was corrected before seal formation. In all recordings, a holding potential of −40 mV was chosen to inactivate Na^+ channels. I_{Ca} or I_{Ba} were activated in response to 100-ms depolarizing voltage steps from −40 to 0 mV. I_{Ca} was measured at 5 s intervals except when electrophysiological measurements were combined with fluorescence measurements at intervals of 25 s. The measured currents were filtered at 1 or 10 kHz, digitized at 10 or 100 kHz, and plotted and analyzed in terms of magnitude and time constants of decay using Graph Prism (GraphPad Corp., San Diego, CA, USA) and pCLAMP 9.0 software.

To study the effects of anoxia on ionic currents, the voltage-clamped single cells were perfused with external solutions equilibrated with atmospheric O_2 (normoxic) or 100% N_2 (hypoxic). Recordings in normoxic or hypoxic solutions were performed in oxygen or nitrogen bubbled solutions. Solution exchange took place within 50 ms using an electronically controlled perfusion system equipped with five barrels loaded with control and hypoxic and Tyrode's solutions containing varying electrolyte concentrations and pharmacological agents [30]. The O_2 pressure was measured with a needle probe which registered < 5 mmHg for the hypoxic solutions both in the bubbled reservoirs and near the port for solution outflow into the main chamber. HEPES (10 mM) was used to buffer the extracellular solutions, which prevented changes in the pH of the external solutions with bubbling of O_2 or N_2. Acidification of the media to pH 6.7, was achieved by addition of isotonic HCl. The pH of all solutions was carefully determined using a pH meter at room temperature (~ 25°C).

Fluorometric Ca^{2+} measurements in voltage-clamped cells

Single isolated beating rN-CMs were subjected to 100 ms depolarizing voltage-clamp pulses (−40 to 0 mV) to activate I_{Ca} and the triggered intracellular Ca^{2+} transient. Intracellular Ca^{2+} signals were measured with the fluorescent Ca^{2+}-indicator dye Fluo-4AM (2 μM, Invitrogen), following 40 min incubation of cells at 37 °C and 5% CO_2. The fluorescence probes were excited at 460 nm using a LED-based illuminator (Prismatix, Modiin Ilite, Israel) and gated aperture and Ca^{2+}-dependent fluorescent light (>500nm) was detected with a photomultiplier tube using a Zeiss Axiovert 100 TV inverted microscope.

Focal Ca^{2+} transients were monitored using genetically engineered virally introduced biosensors GCaMP6-FKBP targeted to FKBP-12.6 (calstabin-2) binding site of RyR2 (K_d=250 nM, λ_{ex}=488 nm). The probe uses calmodulin as Ca^{2+} chelator and green fluorescent protein (GFP) as reporting fluorophor, which allows it to sense the Ca^{2+} in the micro-domains of dyadic clefts where CICR takes place. To examine the mitochondrial Ca^{2+} signaling we developed a genetically engineered mitochondrial Ca^{2+} probe, GCaMP6-cytochrome probe (mito-GCaMP6, K_d=245 nM, λ_{ex}=488 nm). The probe carried

mitochondrial pre-sequence (MPS) and was infected into cultured rN-CM using an adenovirus construct producing confocal fluorescence images characteristic of mitochondrial patterns [31]. For both probes the parameter of the Ca^{2+} signals analyzed was the peak of the Ca^{2+} transient.

Chemical products

Products to make saline solutions, as well as nifedipine and isoprenaline hydrochloride were purchased from Sigma (Sigma-Aldrich, St Louise, MO, USA). Amphotericin B was purchased from Fisher Scientific (Pittsburgh, PA, USA). Stock solution of isoprenaline hydrochloride was prepared in deionized water prepared each experimental day, as was nifedipine and amphotericin B in DMSO. Nifedipine was prepared under dark conditions and the experiments with this photosensitive dihydropyridine were performed under dark conditions (barrel with the drug covered in foil).

Statistical analysis

Data are expressed as means ± standard error of the mean (SEM) of the number of cells and cultures indicated in parentheses (*n, N*). Unpaired two-tailed Student's *t* test was used to compare means. A *P* value equal or smaller than 0.05 was taken as the limit of significance. Significance levels are indicated with an increasing number of asterisks (*$P < 0.05$, **$P < 0.01$, ***$P < 0.001$) and on occasion to be not significant (n.s., $P > 0.05$). Data sets were tested for normality (Kolmogorov-Smirnov normality test), an assumption for the application of the Student's t-test. We found that some groups didn't fit well to normal distributions, a nonparametric statistical test was used (Mann-Whitney's rank sum test to compare two samples). Scatter plot were used to explore the association between cell size or blockade of the I_{Ca} by hypoxia and tau inactivation of the I_{Ca} and the correlations between these variables were analyzed by Pearson linear correlation coefficient. To analyze I_{Ca} decay or *tau inactivation* of the I_{Ca} (τ_i), single exponential fits were applied to the decaying part of individual I_{Ca} traces using a simplex optimization algorithm as follows: $y = y_0 + \{1 - [A_i \exp(- t/\tau_i)]\}$ where A_i represent the amplitudes of the I_{Ca} and τ_i represent the time constants of inactivation respectively. All statistical analysis was performed using GraphPad Prism 7.0 (GraphPad Software, La Jolla, CA) and MS Excel (Microsoft, Redmond, WA).

RESULTS

I: Ca^{2+} channel inactivation kinetics suggests two cell populations

Calcium currents were measured in primary cultures of rN-CM using the perforated-patch mode of the whole-cell patch-clamp technique. Surprisingly we consistently found two distinct cell types based on the inactivation kinetics of I_{Ca}. In one set of cells I_{Ca} inactivated rapidly (τ_i = 12.34 ± 1.62 ms, n=29 cells) while in another set of cells I_{Ca} inactivated slowly (τ_i = 41.96 ± 4.38 ms, n=24 cells), see also Fig. 1A, B. Even though both cell types were observed on every day of culture, the percentage of cells with rapidly inactivating I_{Ca} was consistently higher in the early postnatal days (79.4 % at up to 5 days of culture versus 13.4% at day 7), Fig. 1C. Consistent with this finding, smaller cells (10–30 pF) had predominantly rapidly inactivating I_{Ca}, while cells larger than 40 pF had progressively slower inactivation kinetics (Fig. 1G). Cell size, estimated from measurement of membrane

capacitance increased significantly with culture time, ranging from 13.68 ± 1.07 pF at day 4, to 22.91 ± 1.79 pF at day 5, to 25.44 ± 2.75 pF at day 6 and to 33.40 ± 5.53 pF at day 7, reflecting cell growth. In a similar manner the Ca^{2+} channel current increased significantly, from 74.49 ± 7.57 pA at day 4, to 152.18 ± 19.94 pA at day 5, to 186.1 ± 30.20 pA at day 6 and to 235.7 ± 17.54 pA at day 7 (Fig. 1A, B, D); nevertheless, Ca^{2+} current density did not change significantly (5.54 ± 0.79 pA/pF at day 4, 5.84 ± 0.31 pA/pF at day 5, 7.27 ± 0.84 pA/pF at day 6, and 6.19 ± 0.89 pA/pF at day 7, Fig. 1E). These finding suggests that there was a proportional increase in the number of calcium channels with cell growth in culture.

The distribution of the inactivation time constant (τ_i) of I_{Ca} during 5, 6 and 7 days in culture generated three frequency histograms which could be fit with bell-shaped distributions centered at ~20 ~40 or ~100 ms, respectively (Fig. 1F). Box and colored whiskers plots (blue, red and green) show the distribution of the τ_i for the tree different groups with the median values of 19, 45 and 93 ms, respectively (Fig. 1F). In addition, Fig. 1 G shows that there was a positive linear correlation ($r = 0.653$ $p<0.0001$) between the cell size (pF) and the inactivation time constant of the I_{Ca}. The dotted vertical line at $\tau_i = 35$ ms, Fig.1G, was chosen to denotes approximate separation of the two cell populations (black circles, $\tau \leq 35$ ms) and those with much slower inactivating I_{Ca}.

Since rN-CMs are reported to express both L and T-types of I_{Ca} [32], we tested for the ionic and pharmacological sensitivities of the slowly and rapidly inactivating currents. Pharmacological blocker of L-type I_{Ca}, nifedipine, at 3 μM almost completely and reversibly blocked (85.77 ± 4.75 %, data not shown), both the rapidly and slowly inactivating I_{Ca}. Consistent with the specificity of nifedipine effect on L-type Ca^{2+} channels, 50 μM Ni^{2+}, known to block T-type I_{Ca}, had no suppressive effect on either rapidly or slowly inactivating I_{Ca} (Fig. 2 D, I & J).

The calcium dependent inactivation (CDI) property of both cell types were also consistent with those previously reported for L-type I_{Ca}, as replacing Ca^{2+} with Ba^{2+}, significantly slowed the inactivation kinetics of I_{Ca} in both cell types, slowing the inactivation kinetics of rapidly inactivating I_{Ca} from 14.07 ± 0.89 to 43.80 ± 2.33 ms in Ba^{2+} (data not shown). Similarly, shifting the holding potential from −40mVs to −60mVs failed to recruit any additional current as would be expected from activation of T-type I_{Ca} (Fig. 2E).

To further substantiate that the rapidly inactivating I_{Ca} was carried by the L-type Ca^{2+}channels, 3 μM nifedipine was first used to block almost completely the rapidly inactivating I_{Ca} and then the sensitivity of the remaining current to Ba^{2+} was determined (Fig. 2A, B). Exposure of such cells to 2 mM Ba^{2+} plus nifedipine increased the τ_i from 17.57 ± 4.39 to 48.20 ± 5.83 ms, confirming that L-type Ca^{2+} channels carried the remaining nifedipine-insensitive current (Fig. 2A & C). The almost complete block of both rapidly and slowly inactivating I_{Ca} by nifedipine (Fig. 2B & G) and slowing of the inactivation kinetics of both cell-types by Ba^{2+} (Fig. 2C & H) confirmed that both the slowly and rapidly inactivating I_{Ca} were carried by L-type Ca^{2+} channels. Note that washout of nifedipine fully recovered I_{Ca} within ~ 2 min (Fig. 2A, B, F & G).

II: Hypoxia effects on Neonatal Cardiomyocytes

A. Differential effects of hypoxia on slowly and rapidly inactivating I_{Ca}.—To achieve rapid changes in the extracellular PO_2, the normoxic solution (bubbled with 100% O_2) surrounding the voltage-clamped cell was replaced by a hypoxic solution (bubbled with 100% N_2; PO_2 < 5 mmHg) in less than 1s and I_{Ca} was measured during repeated depolarizations from −40 to 0 mV. Ca^{2+} channel run-down was minimized by the use of perforated-patch clamp approach, which caused little or no significant decrease in I_{Ca} for periods of 3–5 minutes when cells were exposed to only normoxic solutions (Fig. 3C and 3D, open circles). Exposure of such cells to hypoxic solution produced ~10% initial suppression of I_{Ca} within the first 5 s both in cells with rapidly and slowly inactivating I_{Ca}, followed by gradually increasing suppression that stabilizes in 100 s at levels of 20.3 ± 2.6 % (n = 6, N = 4) in cells with rapidly inactivating I_{Ca} (Fig. 3C, filled circles), but at 39.8 ± 8.5 % (n = 9, N = 4) levels in the cells with slowly inactivating I_{Ca} (Fig. 3D, filled circles). In both cell types I_{Ca} recovered to its control levels following the return of normoxic solutions in about 70 s (Fig. 3C and D filled circles, see also original tracing of I_{Ca} in two representative myocytes, Fig. 3A and B).

Comparison of the degree of hypoxic suppression as a function of rate of inactivation of I_{Ca} (scatter-gram, Fig. 3E), even though showing significant variability in the hypoxic suppressive effect, had a positive linear correlation (r = 0.581 p<0.001) between hypoxic suppression of I_{Ca} and the rate of its inactivation. Box and whiskers plots of panel E show that the larger cells had ~2 times larger distribution for slowly (white box) than rapidly inactivating cell (black box) with hypoxia, since the larger cells appeared to express the slower rate of inactivation of I_{Ca} (Fig. 1F), we conclude that hypoxia is more effective in suppressing I_{Ca} in the larger older cells. Fig. 3F shows the average values of the inactivation time constants of I_{Ca} before, during and after exposure to hypoxia for each of the two cell types. In the normoxic control conditions the inactivation τ_i averaged 13.90 ± 1.84 ms for the rapidly inactivating I_{Ca} and 40.87 ± 9.09 ms for the slowly inactivating I_{Ca}. Acute hypoxia appeared to slow the mean rate of the inactivation time constant of I_{Ca}, only in cells with slowly inactivating I_{Ca}, though not significantly ($P > 0.05$).

B. Modulation of phosphorylated I_{Ca} by hypoxia in cells with rapidly or slowly inactivating I_{Ca}—The modulation of the L-type channel by PKA occurs subsequent to a direct phosphorylation of the α1- and the associated β-subunits of the channel [33–34]. Fig. 4 shows that 100 nM isoproterenol (ISO) increased I_{Ca} by 52.45 ± 6.7 % in the cells with rapidly inactivating I_{Ca} (Fig. 4C) and by 60.13 ± 7.2 % in the cells with slowly inactivating I_{Ca} (Fig. 4D). In isoproterenol treated myocytes hypoxia suppressed I_{Ca} by 18.77 ± 7.21 % in cells expressing the rapidly inactivating I_{Ca} (Fig. 4C) and by 53.12 ± 5.28 % in cells with slowly inactivating I_{Ca} (Fig. 4D). The effects of hypoxia were also evaluated on the kinetics of inactivation of I_{Ca} (Fig. 4E and F), but similar to the data in non-phosphorylated control cell, there were no significant effects on τ_i. Thus PKA-mediated phosphorylation did not seem to affect significantly the suppressive effects of hypoxia on I_{Ca}, even though the extent of suppression in two types of cells varied greatly. This finding in rN-CM is somewhat similar to that reported by [35–36] in adult rat cardiomyocytes and in contrast to that reported for adult guinea pig cardiomyocytes [37].

C. Ba^{2+} transporting calcium channels and the hypoxic response—In adult rat cardiomyocytes when Ba^{2+} was used to suppress CDI of Ca^{2+} channels, the effect of acute hypoxia was accentuated from 18% to 35% during the 50s exposure times to hypoxic solutions [35–36]. Figure 5 similarly shows that in neonatal cardiomyocytes when 2 mM Ca^{2+} was replaced by 2 mM Ba^{2+} a fast suppression of I_{Ba} also occurred by hypoxia within the first 5 s in both the rapidly (17.4 ± 1.4 %, Fig. 5C) or slowly (12.8 ± 3.7 %, Fig. 5D) inactivating I_{Ca} cell-types, that was then followed by 45.2 ± 6.2 % and 40.1 ± 1.8 % suppression respectively during a 100 s hypoxic exposure period (Fig. 5A–D).

The kinetics of inactivation of Ica were also attenuated by dialyzing the 4–5 day old myocytes, where rapidly inactivating I_{Ca} cell types predominate, with high concentrations of calcium buffers EGTA (10 mM) and BAPTA (10 mM) using the whole cell configuration of patch clamp technique, fig. S6. As shown in panel A, 11 out of 11 myocytes patched had clear slowly inactivating I_{Ca}, τ_i> 40 ms; (see also insets of the panels C and D, fig. S6). Note that the response to hypoxia (panel A, B and C, fig. S6) was also quite similar to those cells that were described in figure 3 for slowly inactivating I_{Ca} using perforated patch-clamp, with Ca^{2+} as charge carrier (~ 40% suppression of I_{Ca} after 100 seconds of exposure to hypoxia). Interestingly, in this set of cells (mostly small cells, panel D) suppression by hypoxia remains at 40% at τ_i> 40 ms, panel C. In addition, highly Ca^{2+} buffered rN-CMs, under hypoxic conditions, appear to be less sensitive to isoproterenol. (panels A and B fig. S6).

Thus, the slow inactivation of the channel, whether naturally occurring in a population of neonatal myocytes, or induced by high cytosolic Ca^{2+} buffering, or transport of Ba^{2+} through the channel appears to sensitize the channel to hypoxia, as if rapid inactivation of the channel, mediated by CDI, is protective against hypoxia.

III: Hypoxia plus Acidosis effects on Neonatal Cardiomyocytes

A. Effects of acidification and hypoxia on slowly and rapidly inactivating I_{Ca}—Since hypoxia is often accompanied by ischemia, in another set of experiments the combined effects of acute acidification and hypoxia were examined in both cell-types. In cells expressing rapidly inactivating I_{Ca}, acidification (pH 6.7) suppressive effects occurred rapidly and were larger (41.13 ± 5.44 %) compared to ~12% hypoxia-induced suppression (Fig. 6A, B, and C). In sharp contrast, in slowly inactivating I_{Ca} cell-types, where the suppressive effects of acidosis on I_{Ca} amplitude was quite similar (~38%), the suppression developed slowly, but the combined effect of low pH and hypoxia was not additive as it were in rapidly inactivating cells (Fig. 6C, *vs.* 6G).

B. Acidification effects on phosphorylated Ca^{2+} channels—Since ischemia caused by coronary episodes is also accompanied by discharge of adrenergic hormones [38], we examined the effects of acidosis on isoproterenol-treated myocytes. Acidosis (pH=6.7) suppressed the isoproterenol enhanced I_{Ca} in both cell types, but was less effective in slowly inactivating population of cells (~10 % vs. 25.16 ± 5.01 %, Fig. 7 C, D, E), see also scatter-gram of suppression of the I_{Ca} (acidosis + ISO) vs. inactivation time constant (τ_i) for cells with rapidly (●) and slowly (○) inactivating I_{Ca} (Fig. 7F).

To examine whether the lower effectiveness of acidosis in suppressing the phosphorylated channels results solely from increased density of the current through the channel, I_{Ca} was enhanced by increasing the extracellular Ca^{2+} concentration from 2–5 mM. Supplementary figure 1C shows that when I_{Ca} was augmented by 47.92 ± 7.28 % at pH 7.4, equivalent to adrenergic enhancement of the current (Fig. 7C & D), acidosis decreased the potentiated current by 51.53 ± 5.13 % (figure S1A, B, C), somewhat larger than when measured using 2 mM of Ca^{2+} (Fig. 7), and the suppressive effect was equivalent in both cell types. These findings suggest that PKA phosphorylation protects against acidosis-induced suppression by a mechanism other than the simple enhancement of current density, that is, phosphorylation appears to be more protective against ischemia than hypoxia in rN-CM.

C. Acidification effects on calcium and barium transporting calcium channels—We also compared the effect of acidosis on Ba^{2+} versus Ca^{2+} transporting Ca^{2+} channels. Low pH (6.7) solutions only moderately suppressed (14.70 ± 6.57 %) I_{Ba} as compared I_{Ca} (39.91 ± 12.53 %, data not shown). The often-observed modest increase in the time constant of inactivation of Ca^{2+} transporting channels in low pH solutions was also absent in Ba^{2+} transporting channels. These results are consistent with the idea that the H^+ maybe more effective in competing for the permeation site when Ca^{2+} rather than Ba^{2+} is the charge carrier through the channel, consistent with higher permeability of Ba^{2+} through the calcium channel [39–41].

D. Hypoxia and Acidosis effects on global and focal Ca^{2+} Signaling—In the next set of experiments the effects of hypoxia and acidosis on global and focal cytosolic Ca^{2+} transients were measured using Fluo-4 AM for global, GCamP6-FKBP for the focal RyR2 microdomains, and mito-GCaMP6 targeted to mitochondrial matrix to monitor its Ca^{2+} profiles. Hypoxia and acidosis suppressed global cytosolic Ca^{2+} transients, by about 21% and 23%, respectively, in response to 35% and 26% reduction of I_{Ca} respectively (Fig. 8G–L). On the other hand, focal RyR2 Ca^{2+} transients were suppressed to a greater degree by hypoxia (35 %) and acidosis (42 %) using the GCaMP6-FKBP probe (Fig. 8A–F), for equivalent reduction of I_{Ca} of 34% by hypoxia and 23% by acidosis.

The combined effects of hypoxia and acidosis on the global cytosolic Ca^{2+} transients (Fluo-4 signals) were not additive (35% blockade, for 40% suppression of I_{Ca} (figure S3A, B, C). However, the combined effects of hypoxia and acidosis were significantly larger (64%) on focal Ca^{2+} transients measured with GCaMP6-FKBP in response to an equivalent (36 %) reduction in I_{Ca} (figure S3D, E, F).

In another set of cells we dialyzed the cells with high concentrations of HEPES (30 mM) to increase their intrinsic pH buffering capacity, thus attenuating or minimizing the possible intracellular pH changes on decreasing extracellular pH [42]. Fig. S5 shows that lowering the extracellular pH under these conditions continues to suppress the calcium transient amplitude by ~15% and 25% using Fluo4-AM (fig. S4) and GCaMP6-FKBP (fig. S5), respectively. These values were slightly smaller than when perforated patch method was used (~20 % and ~35%) where the buffering capacity is close to that of natural cellular state, but the ratio of suppression of the calcium transient by low pH when using Fluo4-AM and GCaMP6-FKBP (Global/Focal) in both treatments (high HEPES dialysis/no dialysis), is

fairly similar (15/20 Vs 25/35, respectively), suggesting that at least lowering the extracellular pH to 6.7 does not significantly alter the qualitative nature of the results.

Hypoxia but not acidosis strongly suppressed Ca^{2+} uptake into the mitochondrial matrix, respectively by 40 % and 10 %, Fig. 8M–P. Similarly, hypoxia reduced the mitochondrial Ca^{2+} uptake, measured as the rate of rise of mito-GCaMP6 signal (fig. S7). This effect was quantitatively different in the two cell types; it was significant and markedly larger in slowly inactivating I_{Ca} cells –panel B and C fig. S7– (41% versus 15% suppression).

The disparity in hypoxic suppression of cytosolic Ca^{2+} signals when measured by GCaMP6-FKBP (35 %) and Fluo-4 (21 %) may in part reflect the extent to which hypoxia (Fig. 8O & P), but not acidosis (Fig. 8M & N) suppresses mitochondrial Ca^{2+} uptake, thus allowing a higher global cytosolic Ca^{2+} to be detected by Fluo-4. These finding suggest measurements of Ca^{2+} releases using targeted Ca^{2+} probes not only provide a better indicator of ischemic insult, but also suggests that global Ca^{2+} release measurements may have multiple components, reflecting contribution of different cellular Ca^{2+} pools including mitochondria.

DISCUSSION

The novel findings reported here are that rat neonatal cultures of cardiomyocytes express two cell-populations based on the kinetics of inactivation of their L-type Ca^{2+} current: cells expressing rapidly inactivating I_{Ca}, prevalent in 3–4 day cultures, and cells expressing slowly inactivating I_{Ca}, predominantly in 7 day cultures. Hypoxia or acidosis suppressed I_{Ca} in both cell types but to different degrees and with different kinetics. The magnitude of suppression appeared to depend on the rate of inactivation of the channel-i.e. the slower the inactivation, the larger was the hypoxic suppression. The differential hypoxic suppression of I_{Ca} in the two cell types disappeared when Ba^{2+} was the charge carrier through the channels or when the Ca^{2+} buffering capacity of myocytes was increased by high concentrations of EGTA and BAPTA (fig. S6), suggesting that the Ca^{2+}-dependent inactivation protected the channel against hypoxic suppression. In sharp contrast to the enhanced suppressive effects of hypoxia on Ba^{2+} transporting channels, acidosis suppression of I_{Ba} was not significantly altered, suggesting that CDI was unlikely to regulate the ischemic effect. PKA phosphorylation, on the other hand, appeared to protect the channel against acidosis but not hypoxia.

Hypoxia and acidosis also suppressed Ca^{2+} signaling. The suppressive effects on global Ca^{2+}-transients were small and consistent with the suppression of I_{Ca} and thereby affecting CICR. Surprisingly, the suppressive effects of hypoxia were significantly larger in slowly inactivating I_{Ca} cells (*$P < 0.05$ Mann-Whitney rank-sum test) when targeted probes (GCaMP6-FKBP) to RyR2-microdomains were used (compare, Fig. 8A–F, to panels 8G–L), suggesting that multiple pools of Ca^{2+} may contribute to the global rise of Ca^{2+}. Consistent with this idea, the uptake of Ca^{2+} into the mitochondria following SR Ca^{2+} release (measured directly with targeted mito-GCaMP6, Fig. 8 and fig. S7), was strongly suppressed by hypoxia (Fig. 8O, P), but not by acidosis (Fig. 8M, N).

Differential expression of rapidly and slowly inactivating I_{Ca} in neonatal cultures

In the first 5 days of culture, I_{Ca} was small in magnitude as cells expressed predominately a rapidly inactivating L-type I_{Ca} (Fig. 1A, C, D). In older 7-day cultures I_{Ca} was larger and inactivated slower (Fig. 1B, C, D). Developmental changes in I_{Ca} were also reported in rN-CM primary cultures [32], but were attributed to expression of T-type Ca^{2+} channels. The electrophysiological and pharmacological characterization of the rapidly inactivating I_{Ca}, in our cell cultures suggest, however, that the current was carried by L- and not T-type Ca^{2+} channels (Fig. 2). We considered three possibilities for the expression of two kinetically different I_{Ca}: 1) a larger surface to volume ratio in less mature smaller cells as was demonstrated in rN-CMs by Vornanen, 1996 [3] (Fig.1G, filled circles), where Ca^{2+} influx and release would be more effective in activating CDI than in the older cells that are likely to have larger volumes, (Fig.1G, open circles), 2) differential expression of molecular determinants of CDI in developing neonatal cardiomyocytes, and 3) differential expression of $Ca_V1.2$ and $Ca_V1.3$ in younger and older cultures. Since the gating kinetics of both cell groups were equally affected with Ba^{2+} as charge carrier through the channel, it is unlikely that CDI was differentially expressed in the two cell populations. The fairly direct relationship between the size of the cell and rate of I_{Ca} inactivation, Fig. 1G, supports the cell size possibility to be responsible for two cell-type populations. The differential expression of $Ca_V1.2$ and $Ca_V1.3$ could also be a contributing factor, though the density of $Ca_V1.3$ is unlikely to be comparable to that of $Ca_V1.2$, as this channel is predominantly expressed in SA-nodal and conducting myocytes. Our studies checking on the level of expression of $Ca_V1.2$ and $Ca_V1.3$, showed that $Ca_V1.2$ mRNA was significantly higher than $Ca_V1.3$ and without noticeable change in $Ca_V1.3$ levels (data not shown), consistent with a previous report showing that the level of $Ca_V1.3$ decreases postnatally as to become absent in adult rA-CMs [43].

Modulation of calcium channel by hypoxia and acidosis in neonatal cardiomyocytes

Although the effects of hypoxia and acidosis have been explored on I_{Ca} by a number of investigators in adult rat ventricular myocytes, [44–47] little has been reported on the combined effects of these interventions on neonatal cardiomyocytes. While the hypoxic suppressive effects on I_{Ca} were quantitatively different in cells with rapidly or slowly inactivating I_{Ca} (~15% vs. ~40% suppression, respectively, Fig. 3C, D), the suppressive effects of acidosis were equivalents (~40% suppression, Fig. 6) in both cell-types. It was a general finding that the hypoxic suppression of I_{Ca} was larger in cells with slowly inactivating Ca^{2+} current (Fig. 3 & 4). This differential effect of hypoxia was absent when Ba^{2+} was the charge carrier through the Ca^{2+} channel (Fig. 5) or myocytes were dialyzed with high concentrations of EGTA or BAPTA, suggesting that CDI was in part responsible for hypoxic suppression of I_{Ca}. One contributing factor to larger suppressive effects of hypoxia on I_{Ca} in larger slowly inactivating subset of cells maybe the rise of cytosolic Ca^{2+} secondary to strongly compromised uptake of Ca^{2+} by mitochondria, Fig. 8P and fig. S7.

The suppressive effect of acidosis, on the other hand, developed with markedly different kinetics (rapid block in cells with rapidly inactivating I_{Ca}, versus slowly developing suppression in cells with slowly inactivating I_{Ca}, Fig.6B & F). In both cell types, however, there was a rapid initial suppression of I_{Ca} resulting probably from binding of protons to the

Ca^{2+} permeation site of the channel pore [48–50], and/or neutralizing the membrane surface charges and thereby altering the gating of the channel [51–53]. The slowly developing phase of suppression of I_{Ca} may result from very weak but sustained ~0.1 pH units intracellular acidification [54], especially in the perforated patch-clamp experiments [20, 55–56]. Consistent with this idea there was little or no slowly developing phase of suppression of I_{Ca} on acidification in myocytes dialyzed with 10mM HEPES where whole-cell clamped approach was used (figure S2).

While the suppressive effects of hypoxia plus acidosis on I_{Ca} were equivalent (55%) in both cell types (Fig. 6B, C, F, G), there was an additive effect of hypoxia plus acidosis in cells with rapidly inactivating I_{Ca} (but not in slowly inactivating I_{Ca}), suggesting that two different pathways were involved in suppressing I_{Ca} in the rapidly inactivating I_{Ca} cells, for instance: blocking of the channel pore by H^+ (low pH) and activation of heme-oxygenase signalling pathway on O_2 withdrawal [36]. A somewhat similar finding was also reported in the glomus cells of carotid body with alkalization and hypoxia [57].

The rapid and reversible suppression of I_{Ba} with hypoxia (Fig. 5A, B), as also reported for adult rat cardiomyocytes [36, 58], is consistent with the idea that L-type cardiac Ca^{2+} channel can directly sense O_2 by a mechanisms somewhat independent of slower alterations of cellular constituents such as ROS, ADP or ATP. Although the nature of the rapid sensing of O_2 remains somewhat elusive, the finding that heme-oxygenase inhibitors block the suppressive effects of hypoxia on I_{Ca} is consistent with the idea that CaM/CaMKII binding motif of C-carboxyl terminal of calcium channel may bind to heme-oxgenase, thereby allowing the channel to also sense O_2 [36]. Under prolonged hypoxia it is likely that the compromised Ca^{2+} uptake function of mitochondria (Fig. 8) will also contribute to I_{Ca} suppression.

Ischemia and hypoxia modulation of Calcium signalling

In cells incubated in Fluo-4 AM, hypoxia had only a small effect on I_{Ca}-triggered Ca^{2+} release beyond its direct suppressive effect on I_{Ca} and thereby on CICR (Fig. 8I, J, L). In myocytes infected with genetically engineered probes (GCaMP6-FKBP) targeted to RyR_2, however, hypoxia (Fig. 8C, D, F) or acidosis alone (Fig. 8A, B, E) or together (figure S3 D, E, F) strongly suppressed the focal Ca^{2+}-transients associated with μ-domains of RyR2 for equivalent suppression of I_{Ca}. The strong suppression of focal Ca^{2+} signals by hypoxia and/or acidosis, when using targeted probes, was unexpected and suggests that global Ca^{2+}-transients may have multiple determinants and may not reflect the regulation of micro-domains critical to CICR. Possible pH sensitivity of the Ca^{2+} probes as the reason for the disparity of the two signals was considered unlikely as high (30 mM) HEPES concentrations, used to significantly increase the intrinsic buffering capacity of the cells, did not significantly alter the blocking effects of hypoxia or acidosis on the amplitudes of the Ca^{2+} signals in the rapidly and slowly inactivating I_{Ca} cells as compared to those observed in perforated patch-clamp experiments (figures S4 and S5).

Since mitochondrial Ca^{2+} uptake was also suppressed by ~40% by hypoxia (Fig. 8O, P), it is likely that the smaller effect of hypoxia on cytosolic Ca^{2+} transients, as measured with Fluo-4, results from compromised mitochondrial sequestration of Ca^{2+}, Fig. 8 I, J, L.

Consistent with this assertion hypoxia appears to block I_{Ca} by ~30% (Fig. 3C, D), leading to ~ 35% suppression of Ca^{2+} release, as detected in microdomains of RyR2 (Fig. 8C, D, F).

In sharp contrast to acute hypoxia, acute acidosis significantly suppressed both the global and focal Ca^{2+} transients with little effect on mitochondrial uptake transients. Early stages of anoxia have been shown to cause neither depolarization of mitochondrial membrane potential nor a rise in the mitochondria calcium concentration [59], consistent with our data. In chronic hypoxia (minutes), on the other hand, both depolarization of mitochondrial membrane potential and accumulation of matrix Ca^{2+} have been reported [59]. Although the role of mitochondria in beat-to-beat regulation of cytosolic Ca^{2+} remains clouded, some suggesting species dependence [60], there is ample evidence that rN-CMs mitochondria can accumulate significant amounts of Ca^{2+} during spontaneous beating [31, 61–64] and can release calcium rapidly in response to shear stress [65], possibly reflecting the cross-talk between Ca^{2+} handling of SR and mitochondria [66]. To what extent hypoxia or acidosis modulates this interaction remains unknown.

Beta-adrenergic modulation of Ischemic and hypoxic effects

In adult guinea pig ventricular cardiomyocytes, hypoxia was reported to increase the sensitivity of L-type I_{Ca} to β-adrenergic stimulation [37], an effect different than our finding in rN-CM (Fig. 4A, B, C, D), or those in adult rat cardiomyocytes [35–36], where isoproterenol application in hypoxic conditions had an equivalent suppressive effect on I_{Ca} (Fig. 4A, B, C, D). On the other hand, phosphorylation appeared to protect the calcium channel against acidosis (about 40 % suppression of I_{Ca} in control vs. ~15% suppression in presence of ISO at pH 6.7, Fig. 7), consistent with the effects found in adult guinea pig ventricular cardiomyocytes where the suppression of I_{Ca} by ischemia was abolished by ISO [67]. Acidosis not only blocks I_{Ca} but also may modulate the channel by decreasing the β-adrenergic receptor numbers and thereby the adenylate cyclase activity as shown in neonatal rabbit hearts [22]. In guinea pig cardiomyocytes, interleukin 1 increases the effects of isoproterenol on I_{Ca} that was suppressed by acidosis through an increase in Na^+/H^+ exchanger activity and activation of a second messenger pathway involving PKC [24]. A differential modulation of these intracellular signalling pathways, or different activity levels of Na^+/H^+ exchanger in the two cell types maybe the cause of this differential effect of adrenergic effect, as isoproterenol mostly prevented the suppressive effect of acidosis on I_{Ca} in slowly inactivating I_{Ca} cells (Fig. 7).

Physiological implications and insights

Our studies on rat neonatal cardiomyocytes not only show two myocyte populations based on inactivation kinetics of I_{Ca}, but also variable effects of hypoxia, but not acidosis, on the two cell types. What contributes to the heterogeneity of I_{Ca} kinetics in the two cell populations remains somewhat unclear. Our studies point to the likelihood that the proximity of SR Ca^{2+} pools to the sarcolemmal Ca^{2+} channel proteins is critical determining factor in the variability of inactivation kinetics [4–5], see also the schematic 1 below. In support of this idea we found that the larger/older cells show progressively slower inactivation kinetics (Fig. 1). The rapidly inactivating smaller cell appear to respond to acute hypoxia in a manner quite similar to adult rat cardiomyocytes [35] with respect to both the magnitude and speed

of suppression of I_{Ca}, consistent with the proposed O_2-sensing mechanism operating through interaction of heme-oxygenase with CaM/CaMKII of the channel moiety [36]. The larger cells, with slower I_{Ca} inactivation kinetics, appeared to be more sensitive to hypoxia, an effect possibly related to compromised mitochondrial sequestration of Ca^{2+}. The hypoxia-induced suppression of Ca^{2+} uptake by mitochondria is greater in slowly inactivating I_{Ca} cells (table 1), and the rate of rise of Ca^{2+} transients is suppressed more significantly by hypoxia in slowly inactivating I_{Ca} cells (panel B and C fig. S7).

The rapid Ca^{2+} dependent inactivation of I_{Ca} appears to be a protective mechanism against hypoxia, as in its absence hypoxia strongly suppresses the channel current whether the charge carrier is Ca^{2+} or Ba^{2+}. While ischemia effects on I_{Ca} take place rapidly and seems to be limited to suppression of CICR, the hypoxia effect have multiple components that include rapid O_2 sensing by calcium channel via CaM/CaMKII/heme-oxygenase signaling as well as the state of mitochondrial Ca^{2+} signaling.

Supplementary Material

Refer to Web version on PubMed Central for supplementary material.

Acknowledgments

This work was supported by National Institute grants to MM: (1) NIHR01 HL15162; (2) R01 HL107600. We thank Dr. XH Zhang for preparation of neonatal cardiomyocytes cultures, Dr. Yuyu Yao for mRNA studies on CaV 1.2 and 1.3, and Cassandra Clift for general technical help and editing.

GLOSSARY

I_{Ca}
calcium current

rN-CM
neonatal rat ventricular cardiomyocytes

rA-CM
adult rat ventricular cardiomyocytes

SR
sarcoplasmic reticulum

RYR
ryanodine receptor

ISO
Isoproterenol

ROS
reactive oxygen species

CICR

calcium-induced calcium release

CDI
calcium-dependent inactivation

mito-GCaMP6 and FKBP-GCaMP6
mitochondrial- and RyR2-targeted Ca^{2+} biosensors

$[Ca^{2+}]_e$
extracellular calcium-concentration

References

1. Rosa AO, Movafagh S, Cleemann L, Morad M. Hypoxic regulation of cardiac Ca2+ channel: possible role of haem oxygenase. J Physiol. 2012; 590(17):4223–37. [PubMed: 22753548]
2. Rosa AO, Yamaguchi N, Morad M. Mechanical regulation of native and the recombinant calcium channel. Cell Calcium. 2013; 53(4):264–74. [PubMed: 23357406]
3. Vornanen M. Contribution of sarcolemmal calcium current to total cellular calcium in postnatally developing rat heart. Cardiovasc Res. 1996; 32(2):400–10. [PubMed: 8796128]
4. Snopko RM, Aromolaran AS, Karko KL, Ramos-Franco J, Blatter LA, Mejia-Alvarez R. Cell culture modifies Ca2+ signaling during excitation-contraction coupling in neonate cardiac myocytes. Cell Calcium. 2007; 41(1):13–25. [PubMed: 16908061]
5. Ziman AP, Gomez-Viquez NL, Bloch RJ, Lederer WJ. Excitation-contraction coupling changes during postnatal cardiac development. J Mol Cell Cardiol. 2010; 48(2):379–86. [PubMed: 19818794]
6. Kamiya K, Guo W, Yasui K, Toyama J. Hypoxia inhibits the changes in action potentials and ion channels during primary culture of neonatal rat ventricular myocytes. J Mol Cell Cardiol. 1999; 31(9):1591–8. [PubMed: 10471343]
7. Stern MD, Silverman HS, Houser SR, Josephson RA, Capogrossi MC, Nichols CG, Lederer WJ, Lakatta EG. Anoxic contractile failure in rat heart myocytes is caused by failure of intracellular calcium release due to alteration of the action potential. Proc Natl Acad Sci U S A. 1988; 85(18): 6954–8. [PubMed: 3413129]
8. Goncalves H, Pinto P, Silva M, Ayres-de-Campos D, Bernardes J. Toward the improvement in fetal monitoring during labor with the inclusion of maternal heart rate analysis. Med Biol Eng Comput. 2016; 54(4):691–9. [PubMed: 26219610]
9. Stanek J. Association of coexisting morphological umbilical cord abnormality and clinical cord compromise with hypoxic and thrombotic placental histology. Virchows Arch. 2016; 468(6):723–32. [PubMed: 26983702]
10. Nock ML, Difiore JM, Arko MK, Martin RJ. Relationship of the ventilatory response to hypoxia with neonatal apnea in preterm infants. J Pediatr. 2004; 144(3):291–5. [PubMed: 15001929]
11. Poets CF, Samuels MP, Southall DP. Epidemiology and pathophysiology of apnoea of prematurity. Biol Neonate. 1994; 65(3–4):211–9. [PubMed: 8038285]
12. Lagercrantz H, Bistoletti P. Catecholamine release in the newborn infant at birth. Pediatr Res. 1977; 11(8):889–93. [PubMed: 887309]
13. Slotkin TA, Seidler FJ. Adrenomedullary catecholamine release in the fetus and newborn: secretory mechanisms and their role in stress and survival. J Dev Physiol. 1988; 10(1):1–16. [PubMed: 3280659]
14. Fernandez-Morales JC, Padin JF, Arranz-Tagarro JA, Vestring S, Garcia AG, de Diego AM. Hypoxia-elicited catecholamine release is controlled by L-type as well as N/PQ types of calcium channels in rat embryo chromaffin cells. Am J Physiol Cell Physiol. 2014; 307(5):C455–65. [PubMed: 24990647]

15. Saegusa N, Moorhouse E, Vaughan-Jones RD, Spitzer KW. Influence of pH on Ca(2)(+) current and its control of electrical and Ca(2)(+) signaling in ventricular myocytes. J Gen Physiol. 2011; 138(5):537–59. [PubMed: 22042988]
16. Konnerth A, Lux HD, Morad M. Proton-induced transformation of calcium channel in chick dorsal root ganglion cells. J Physiol. 1987; 386:603–33. [PubMed: 2445970]
17. Hattori T, Chen J, Harding AM, Price MP, Lu Y, Abboud FM, Benson CJ. ASIC2a and ASIC3 heteromultimerize to form pH-sensitive channels in mouse cardiac dorsal root ganglia neurons. Circ Res. 2009; 105(3):279–86. [PubMed: 19590043]
18. Schelling JR, Abu Jawdeh BG. Regulation of cell survival by Na+/H+ exchanger-1. Am J Physiol Renal Physiol. 2008; 295(3):F625–32. [PubMed: 18480176]
19. Watson CL, Gold MR. Effect of intracellular and extracellular acidosis on sodium current in ventricular myocytes. Am J Physiol. 1995; 268(4 Pt 2):H1749–56. [PubMed: 7733379]
20. Kaibara M, Kameyama M. Inhibition of the calcium channel by intracellular protons in single ventricular myocytes of the guinea-pig. J Physiol. 1988; 403:621–40. [PubMed: 2855346]
21. Fabiato A, Fabiato F. Myofilament-generated tension oscillations during partial calcium activation and activation dependence of the sarcomere length-tension relation of skinned cardiac cells. J Gen Physiol. 1978; 72(5):667–99. [PubMed: 739258]
22. Nakanishi T, Okuda H, Kamata K, Seguchi M, Nakazawa M, Takao A. Influence of acidosis on inotropic effect of catecholamines in newborn rabbit hearts. Am J Physiol. 1987; 253(6 Pt 2):H1441–8. [PubMed: 2827507]
23. Rozanski GJ, Witt RC. Acidosis masks beta-adrenergic control of cardiac L-type calcium current. J Mol Cell Cardiol. 1995; 27(9):1781–8. [PubMed: 8523439]
24. Rozanski GJ, Witt RC. Interleukin-1 enhances beta-responsiveness of cardiac L-type calcium current suppressed by acidosis. Am J Physiol. 1994; 267(4 Pt 2):H1361–7. [PubMed: 7524364]
25. Zhang XH, Wei H, Saric T, Hescheler J, Cleemann L, Morad M. Regionally diverse mitochondrial calcium signaling regulates spontaneous pacing in developing cardiomyocytes. Cell Calcium. 2015
26. Lindau M, Fernandez JM. A patch-clamp study of histamine-secreting cells. J Gen Physiol. 1986; 88(3):349–68. [PubMed: 2428921]
27. Horn R, Marty A. Muscarinic activation of ionic currents measured by a new whole-cell recording method. J Gen Physiol. 1988; 92(2):145–59. [PubMed: 2459299]
28. Aggett PJ, Fenwick PK, Kirk H. The effect of amphotericin B on the permeability of lipid bilayers to divalent trace metals. Biochim Biophys Acta. 1982; 684(2):291–4. [PubMed: 7055571]
29. Rae J, Cooper K, Gates P, Watsky M. Low access resistance perforated patch recordings using amphotericin B. J Neurosci Methods. 1991; 37(1):15–26. [PubMed: 2072734]
30. Cleemann L, Morad M. Role of Ca2+ channel in cardiac excitation-contraction coupling in the rat: evidence from Ca2+ transients and contraction. J Physiol. 1991; 432:283–312. [PubMed: 1653321]
31. Haviland S, Cleemann L, Kettlewell S, Smith GL, Morad M. Diversity of mitochondrial Ca(2)(+) signaling in rat neonatal cardiomyocytes: evidence from a genetically directed Ca(2)(+) probe, mitycam-E31Q. Cell Calcium. 2014; 56(3):133–46. [PubMed: 24994483]
32. Gomez JP, Potreau D, Branka JE, Raymond G. Developmental changes in Ca2+ currents from newborn rat cardiomyocytes in primary culture. Pflugers Arch. 1994; 428(3–4):241–9. [PubMed: 7816546]
33. Hulme JT, Westenbroek RE, Scheuer T, Catterall WA. Phosphorylation of serine 1928 in the distal C-terminal domain of cardiac CaV1.2 channels during beta1-adrenergic regulation. Proc Natl Acad Sci U S A. 2006; 103(44):16574–9. [PubMed: 17053072]
34. Haase H, Bartel S, Karczewski P, Morano I, Krause EG. In-vivo phosphorylation of the cardiac L-type calcium channel beta-subunit in response to catecholamines. Mol Cell Biochem. 1996; 163–164:99–106.
35. Movafagh S, Morad M. L-type calcium channel as a cardiac oxygen sensor. Ann N Y Acad Sci. 2010; 1188:153–8. [PubMed: 20201898]
36. Rosa AO, Movafagh S, Cleemann L, Morad M. Hypoxic regulation of cardiac Ca2+ channel: possible role of haem oxygenase. J Physiol. 2012; 590(Pt 17):4223–37. [PubMed: 22753548]

37. Hool LC. Hypoxia alters the sensitivity of the L-type Ca(2+) channel to alpha-adrenergic receptor stimulation in the presence of beta-adrenergic receptor stimulation. Circ Res. 2001; 88(10):1036–43. [PubMed: 11375273]
38. O'Connell TD, Jensen BC, Baker AJ, Simpson PC. Cardiac alpha1-adrenergic receptors: novel aspects of expression, signaling mechanisms, physiologic function, and clinical importance. Pharmacol Rev. 2014; 66(1):308–33. [PubMed: 24368739]
39. Ertel SI, Ertel EA, Clozel JP. T-type Ca2+ channels and pharmacological blockade: potential pathophysiological relevance. Cardiovasc Drugs Ther. 1997; 11(6):723–39. [PubMed: 9512867]
40. Fenwick EM, Marty A, Neher E. Sodium and calcium channels in bovine chromaffin cells. J Physiol. 1982; 331:599–635. [PubMed: 6296372]
41. Saimi Y, Kung C. Are ions involved in the gating of calcium channels? Science. 1982; 218(4568): 153–6. [PubMed: 6289432]
42. Swietach P, Camelliti P, Hulikova A, Kohl P, Vaughan-Jones RD. Spatial regulation of intracellular pH in multicellular strands of neonatal rat cardiomyocytes. Cardiovasc Res. 2010; 85(4):729–38. [PubMed: 19828673]
43. Qu Y, Karnabi E, Ramadan O, Yue Y, Chahine M, Boutjdir M. Perinatal and postnatal expression of Cav1.3 alpha1D Ca(2)(+) channel in the rat heart. Pediatr Res. 2011; 69(6):479–84. [PubMed: 21378599]
44. Poole-Wilson PA. Acidosis and contractility of heart muscle. Ciba Found Symp. 1982; 87:58–76. [PubMed: 6804193]
45. Orchard CH, Cingolani HE. Acidosis and arrhythmias in cardiac muscle. Cardiovasc Res. 1994; 28(9):1312–9. [PubMed: 7954638]
46. Komukai K, Pascarel C, Orchard CH. Compensatory role of CaMKII on ICa and SR function during acidosis in rat ventricular myocytes. Pflugers Arch. 2001; 442(3):353–61. [PubMed: 11484765]
47. Komukai K, Brette F, Pascarel C, Orchard CH. Electrophysiological response of rat ventricular myocytes to acidosis. Am J Physiol Heart Circ Physiol. 2002; 283(1):H412–22. [PubMed: 12063316]
48. Prod'hom B, Pietrobon D, Hess P. Interactions of protons with single open L-type calcium channels. Location of protonation site and dependence of proton-induced current fluctuations on concentration and species of permeant ion. J Gen Physiol. 1989; 94(1):23–42. [PubMed: 2553858]
49. Krafte DS, Kass RS. Hydrogen ion modulation of Ca channel current in cardiac ventricular cells. Evidence for multiple mechanisms. J Gen Physiol. 1988; 91(5):641–57. [PubMed: 2458428]
50. Klockner U, Isenberg G. Calcium channel current of vascular smooth muscle cells: extracellular protons modulate gating and single channel conductance. J Gen Physiol. 1994; 103(4):665–78. [PubMed: 8057083]
51. Katzka DA, Morad M. Properties of calcium channels in guinea-pig gastric myocytes. J Physiol. 1989; 413:175–97. [PubMed: 2557436]
52. Ohmori H, Yoshii M. Surface potential reflected in both gating and permeation mechanisms of sodium and calcium channels of the tunicate egg cell membrane. J Physiol. 1977; 267(2):429–63. [PubMed: 17734]
53. Iijima T, Ciani S, Hagiwara S. Effects of the external pH on Ca channels: experimental studies and theoretical considerations using a two-site, two-ion model. Proc Natl Acad Sci U S A. 1986; 83(3): 654–8. [PubMed: 2418439]
54. Matsuda N, Mori T, Nakamura H, Shigekawa M. Mechanisms of reoxygenation-induced calcium overload in cardiac myocytes: dependence on pHi. J Surg Res. 1995; 59(6):712–8. [PubMed: 8538170]
55. Irisawa H, Sato R. Intra- and extracellular actions of proton on the calcium current of isolated guinea pig ventricular cells. Circ Res. 1986; 59(3):348–55. [PubMed: 2429781]
56. Klockner U, Isenberg G. Intracellular pH modulates the availability of vascular L-type Ca2+ channels. J Gen Physiol. 1994; 103(4):647–63. [PubMed: 8057082]
57. Summers BA, Overholt JL, Prabhakar NR. CO(2) and pH independently modulate L-type Ca(2+) current in rabbit carotid body glomus cells. J Neurophysiol. 2002; 88(2):604–12. [PubMed: 12163513]

58. Scaringi JA, Rosa AO, Morad M, Cleemann L. A new method to detect rapid oxygen changes around cells: how quickly do calcium channels sense oxygen in cardiomyocytes? J Appl Physiol (1985). 2013; 115(12):1855–61. [PubMed: 24157525]

59. Di Lisa F, Blank PS, Colonna R, Gambassi G, Silverman HS, Stern MD, Hansford RG. Mitochondrial membrane potential in single living adult rat cardiac myocytes exposed to anoxia or metabolic inhibition. J Physiol. 1995; 486(Pt 1):1–13. [PubMed: 7562625]

60. Griffiths EJ. Species dependence of mitochondrial calcium transients during excitation-contraction coupling in isolated cardiomyocytes. Biochem Biophys Res Commun. 1999; 263(2):554–9. [PubMed: 10491330]

61. Robert V, Gurlini P, Tosello V, Nagai T, Miyawaki A, Di Lisa F, Pozzan T. Beat-to-beat oscillations of mitochondrial [Ca2+] in cardiac cells. EMBO J. 2001; 20(17):4998–5007. [PubMed: 11532963]

62. Drago I, De Stefani D, Rizzuto R, Pozzan T. Mitochondrial Ca2+ uptake contributes to buffering cytoplasmic Ca2+ peaks in cardiomyocytes. Proc Natl Acad Sci U S A. 2012; 109(32):12986–91. [PubMed: 22822213]

63. Bassani RA, Shannon TR, Bers DM. Passive Ca2+ binding in ventricular myocardium of neonatal and adult rats. Cell Calcium. 1998; 23(6):433–42. [PubMed: 9924635]

64. Fieni F, Lee SB, Jan YN, Kirichok Y. Activity of the mitochondrial calcium uniporter varies greatly between tissues. Nat Commun. 2012; 3:1317. [PubMed: 23271651]

65. Belmonte S, Morad M. Shear fluid-induced Ca2+ release and the role of mitochondria in rat cardiac myocytes. Ann N Y Acad Sci. 2008; 1123:58–63. [PubMed: 18375577]

66. Dorn GW 2nd, Maack C. SR and mitochondria: calcium cross-talk between kissing cousins. J Mol Cell Cardiol. 2013; 55:42–9. [PubMed: 22902320]

67. Ross JL, Howlett SE. Beta-adrenoceptor stimulation exacerbates detrimental effects of ischemia and reperfusion in isolated guinea pig ventricular myocytes. Eur J Pharmacol. 2009; 602(2–3): 364–72. [PubMed: 19056376]

Highlights

- Rat neonatal cardiomyocytes cultures express two cell-type populations based on inactivation kinetics of L-type I_{Ca} (tau 10ms & 40ms).
- Acute hypoxia suppressed Ica to varied extent and kinetics in both cell-types, but this effect disappeared when Ba^{2+} was the channel charge carrier or when the intracellular Ca^{2+} buffering capacity was increased, suggesting critical role for Ca^{2+}-dependent inactivation in the hypoxic response.
- Suppressive effect of acute acidosis on I_{Ca} was not cell-type dependent, and was reversed by isoproterenol, but the hypoxic suppression was not reversed by isoproterenol.
- The suppressive effect of Hypoxia on Ca^{2+}-signaling at RyR2 microdomains was significantly larger than that measured in global cytosolic space.
- Hypoxia but not acidosis strongly suppressed mitochondrial Ca^{2+} uptake, suggesting that a component hypoxic suppression of I_{Ca} is related to higher levels of cytosolic Ca^{2+} caused by compromised mitochondrial Ca^{2+} uptake

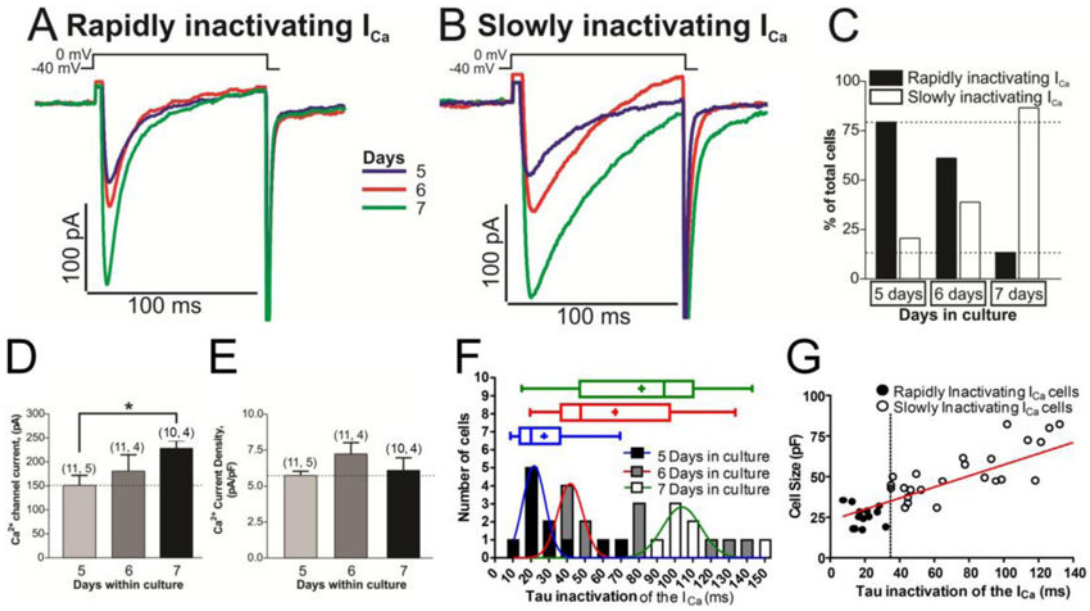

Fig. 1. Two different time dependent kinetics of L-type calcium channels are expressed in cultured rN-CM

Panels A and B show examples of original traces of calcium currents obtained from different rN-CMs with variable ages in culture (5–7 days), activated by depolarization from −40 mV to 0 mV, exhibiting different rates of inactivation: Rapidly inactivating I_{Ca} (Panel A) and slowly inactivating I_{Ca} (Panel B). Panel C shows a plot of the cell percentages that presented rapidly or slowly inactivating I_{Ca} vs. the age of the cells in culture. Panel D and E plotted the average values of I_{Ca} and the Ca^{2+} current density respectively vs. the time of the cells in culture (5–7 days). Panel F provide frequency histograms and box and whiskers plots showing the distribution of the inactivation time constant of the I_{Ca} (τ) at the tree different time in culture (5, 6 and 7 days). The data were pooled in such a way that the number of observations with 0.00 ms ≤ τ_i < 10.00 ms were plotted in the column τ_i = 10 ms. The data were fitted to a Normal Distribution with three different colors Gauss curve represented (blue, red or green for rN-CMs with 5, 6 or 7 days in culture respectively). Data distribution are presented also in box-and-whiskers plots: the line inside the box depicts median values, the size of the box is given by the distance between the 25th and the 75th percentiles; upper "whisker" reach the 90th percentile and lower "whisker" the percentile 10th. Means are also represented inside the box with a cross symbol. Panel G shows a scatter-gram of cell size (pF) vs. inactivation time constant (τ_i) from rN-CMs with rapidly (●) and slowly (○) inactivating I_{Ca}, rN-CMs were classified as expressing rapidly- (τ_i ≤ 35 ms) or slowly-inactivating (τ_i > 35 ms) L-type Ca^{2+} channels.

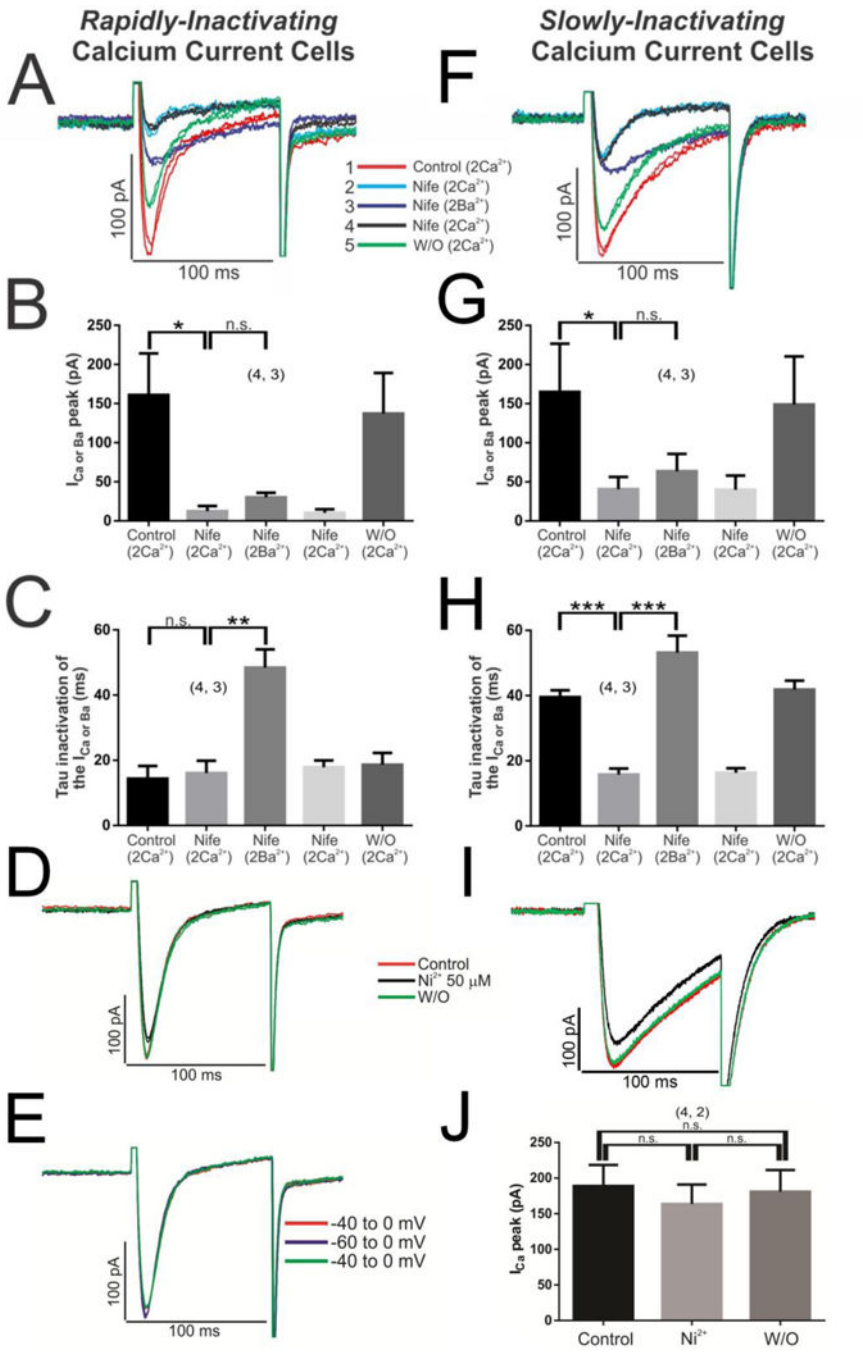

Fig. 2. The rapidly inactivating I_{Ca} is carried by the L-type Ca^{2+} channels and not by T-type

Initially the cells with rapidly inactivating I_{Ca} were perfused with 3 μM nifedipine (blue line-Nife, 2 Ca^{2+}), which reduced almost all of the I_{Ca} signal (Panels A, B); then the perfusion solution was changed with 2 mM Ba^{2+} (instead of Ca^{2+}) maintaining the drug nifedipine (purple line-Nife, 2 Ba^{2+}) which in turn modified the τ_i of the I_{Ba} (Panels A, C); the subsequent return to the previous nifedipine-Ca^{2+} solution (black line-Nife, 2 Ca^{2+}) again reverses the characteristics of the I_{Ca} (Panels A–C). The same set of experiments was conducted in cells with slowly inactivating I_{Ca} (Panels F–H). 50 μM Ni^{2+} was used to block

T-type calcium channels in rN-CMs with rapidly (Panel D) or slowly inactivating I_{Ca} (Panel I). Panel E, shift of the voltage depolarization −40 to −60 mV to recruit possible T-type calcium channels. The duration of each different experimental conditions was 100 s with nifedipine, where the wash/out was extended for 2–3 minutes, nickel where the steady-state was reached in 30 seconds or the experiments with different holding potential (−40/−60 mVs) where the protocol extended only by 15 s.

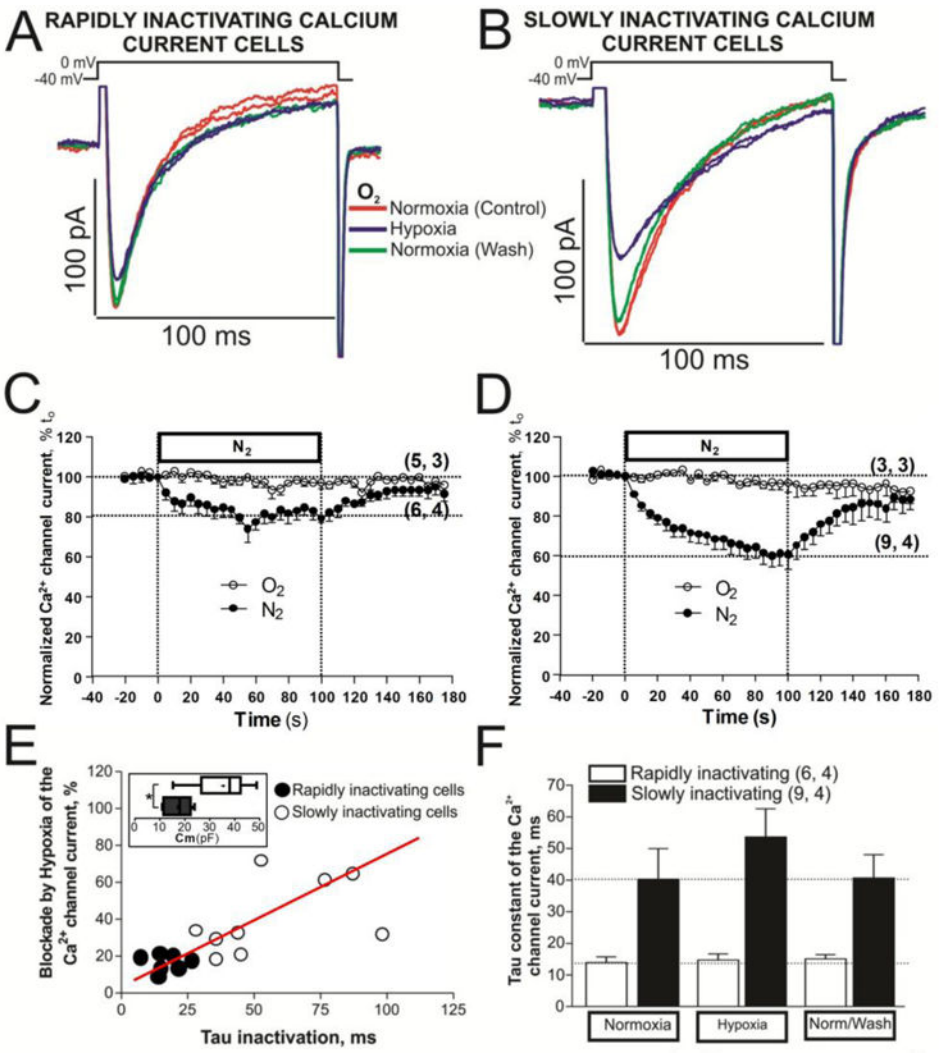

Fig. 3. Acute hypoxia differentially affects to the neonatal cardiomyocytes with rapidly or slowly inactivating I_{Ca}

Panels A and B show examples of original traces of calcium currents obtained from two different rN-CMs, activated by depolarization from −40 mV to 0 mV, exhibiting different rates of inactivation as well as differing degrees of suppression during acute hypoxia (purple traces). Panels C and D display time courses of suppression of I_{Ca} during 2 minutes of hypoxia stimulus (N_2 top bar with filled circles) in rN-CMs with rapidly and slowly inactivating $I_{Ca,}$ respectively. Time courses with open circles represent a set of rN-CMs under normoxic condition during 200 seconds. Panel E shows a scatter-gram of hypoxic suppression of I_{Ca} vs. inactivation time constant (**τ**) from rN-CMs with rapidly (●) and slowly (○) inactivating I_{Ca}. Box and whiskers plots inscribed in the panel E show the distribution of the sell size for the rapidly (black box) and slowly (white box) inactivating rN-CMs. Panel F plotted the average **τ** values of I_{Ca} before, during, and after exposure to hypoxia for each of the two cell types.

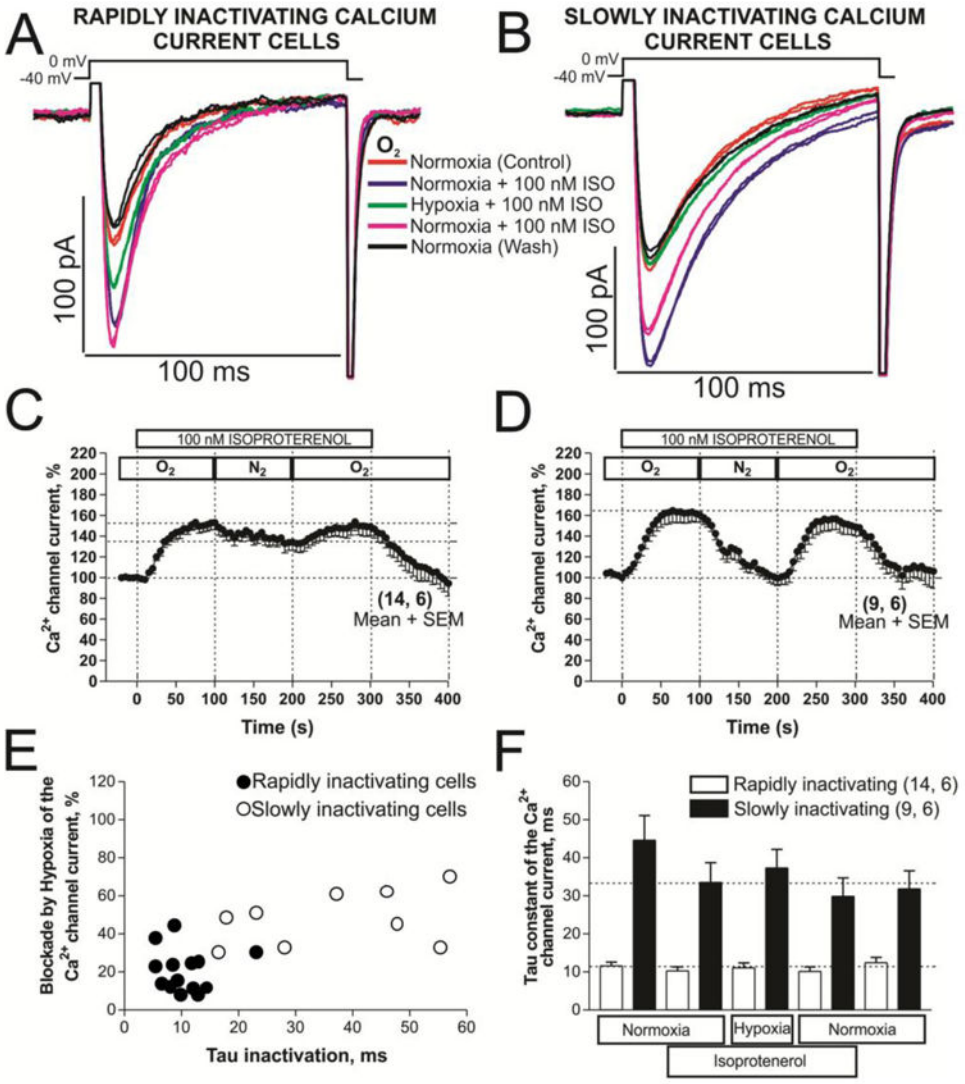

Fig. 4. Phosphorylation effects of isoproterenol (ISO) on calcium channels of rN-CMs with rapidly or slowly inactivating I_{Ca} in normoxia and hypoxia conditions

Panels A and B show examples of original traces of rapidly and slowly inactivating I_{Ca} respectively, obtained from two different rN-CMs, activated by depolarization from −40 mV to 0 mV and exposed to the following consecutive treatments: 1) red traces, normoxia control condition; 2) purple traces, initial treatment with 100 nM ISO in normoxia; 3) green traces, shift to the hypoxic condition maintaining the ISO treatment; 4) pink traces, return to the condition described in 2); 5) black traces, back to the initial normoxia control condition without ISO. Panels C and D displayed time courses (in rN-CMs with rapidly and slowly inactivating $I_{Ca,}$ respectively) of modulation of I_{Ca} by ISO perfused during 5 minutes (ISO bar) at the consecutives conditions of normoxia, hypoxia, and normoxia washout represented by the sequence of O_2, N_2, and O_2 top bars, respectively. Panel E shows a scatter-gram of hypoxic suppression of I_{Ca} vs. inactivation time constant (τ) from rN-CMs with rapidly (●) and slowly (○) inactivating I_{Ca}. Panel F plotted the average τ values of I_{Ca} before, during and after exposure to ISO and hypoxia for each of the two cell types.

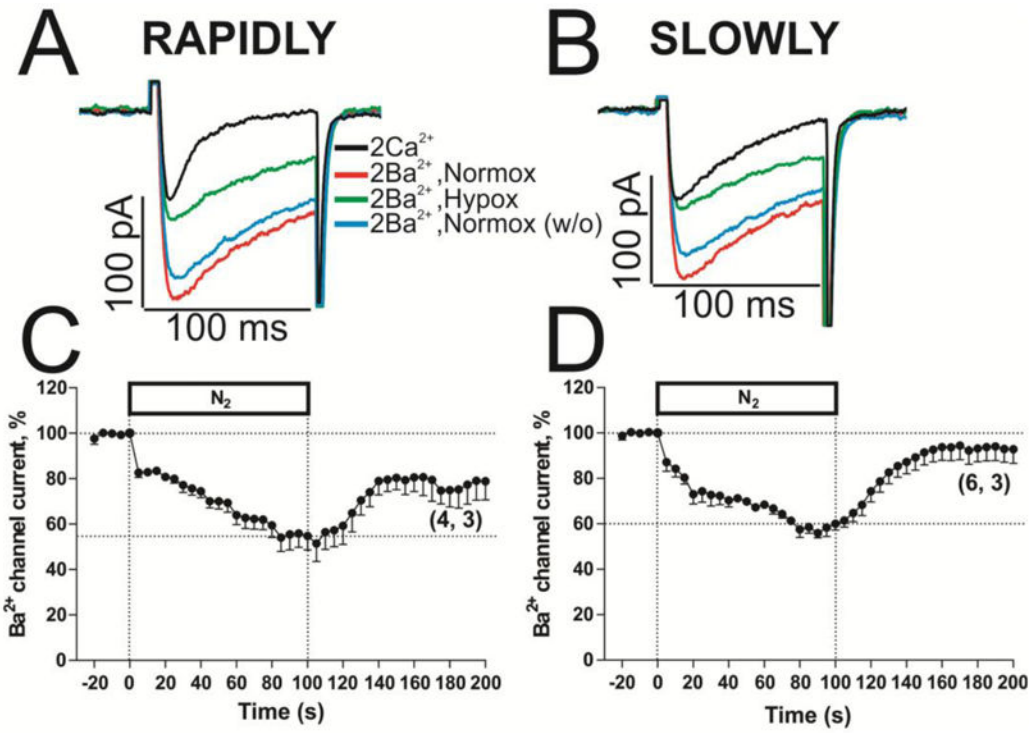

Fig. 5. Cardiac L-type Ca^{2+} channel is more supressed by acute hypoxia when Ca^{2+} is substituted by Ba^{2+} as charge carrier

Panels A and B show examples of original traces of slowly inactivating I_{Ba} from rN-CMs, activated by depolarization from −40 mV to 0 mV and exposed to normoxia (red traces), acute hypoxia (green traces) and normoxia washout (blue traces). Panel C and D displayed the time courses of suppression of I_{Ba} during 100 s by hypoxia stimulus (N_2 top bar) in rN-CMs with rapidly or slowly inactivating I_{Ca} respectively.

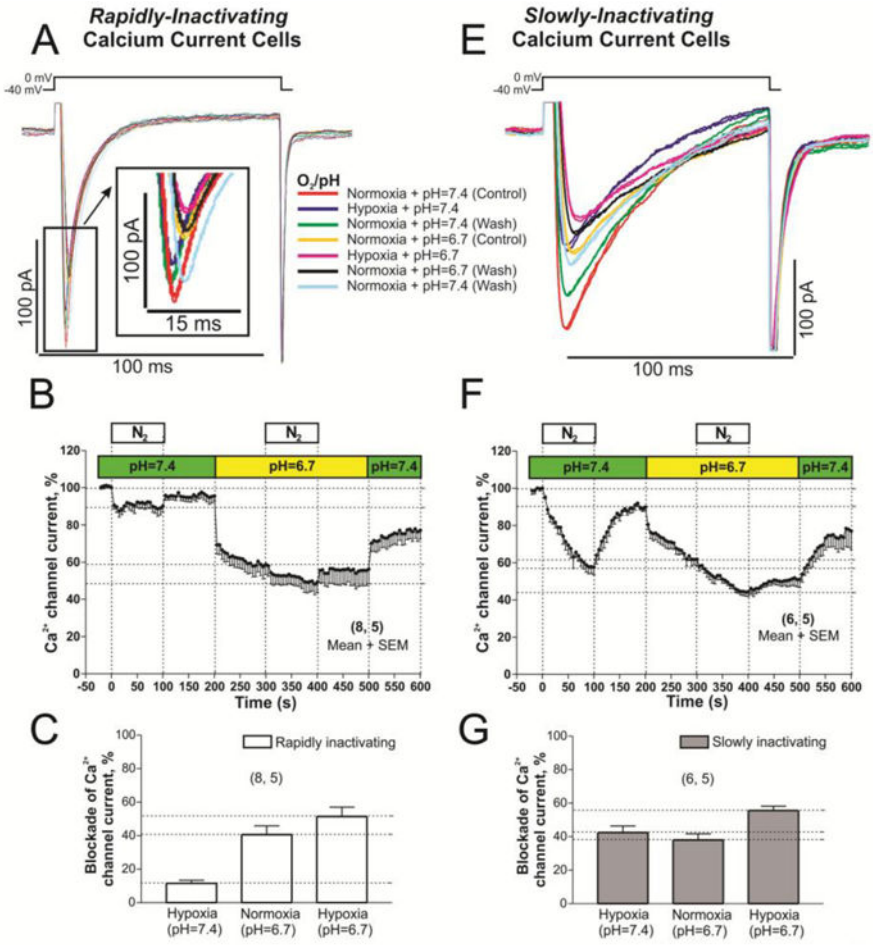

Fig. 6. L-type Ca^{2+} channel is differentially blocked in rN-CMs with rapidly or slowly inactivating I_{Ca} when the stimulus of acute hypoxia and acidification are combined

Panels A and E show examples of original traces of rapidly and slowly inactivating I_{Ca} respectively, obtained from two different rN-CMs, activated by depolarization from −40 mV to 0 mV and exposed to the following consecutive treatments: 1) red traces, normoxia and pH (7.4) control condition; 2) purple traces, hypoxia and control pH 7.4; 3) green traces, back to the initial control treatment (normoxia and pH 7.4); 4) yellow traces, normoxia and low pH 6.7; 5) pink traces, hypoxia and low pH; 6) black traces, again back to normoxia and low pH; 7) blue traces, washout period to normoxia and pH 7.4. Panels B and F displayed time courses (in rN-CMs with rapidly and slowly inactivating I_{Ca} respectively) of the I_{Ca} suppression by low pH (pH=6.7 bar) and/or hypoxia (N_2 bar). Panels C and G plotted the average of I_{Ca} blockade values by hypoxia, low pH, and both stimulus together.

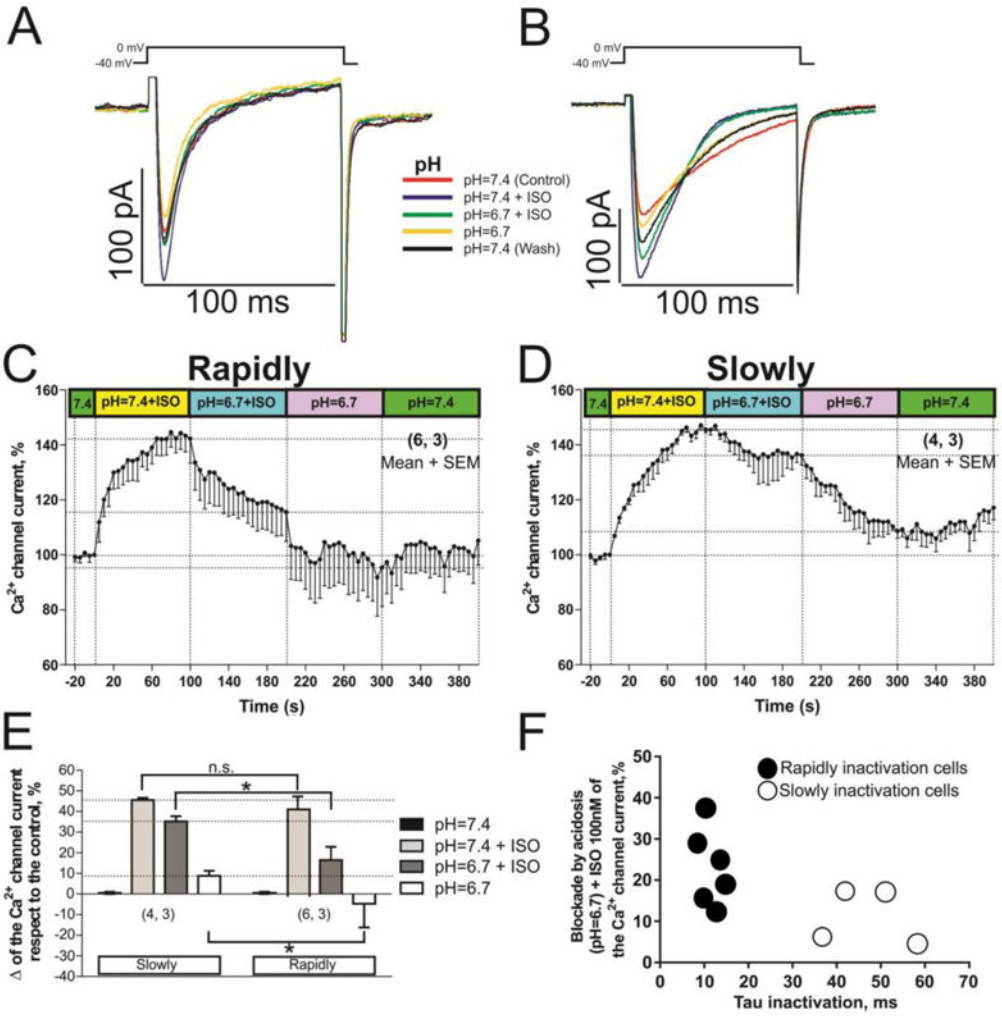

Fig. 7. Acidification effects on calcium channels of rN-CMs with rapidly or slowly inactivating I_{Ca} phosphorylated by ISO

Panels A and B show examples of original records of rapidly and slowly inactivating I_{Ca} respectively, acquired from two different rN-CMs exposed to the next consecutive treatments: 1) red traces, control condition (pH 7.4); 2) blue traces, initial treatment with 100 nM ISO in control pH 7.4; 3) green traces, shift to the low pH condition (6.7) maintaining the ISO treatment; 4) yellow traces, ISO withdrawal and maintenance of the acidic pH; 5) black traces, washout period to control pH 7.4 without ISO. Panels C and D displayed time courses (in rN-CMs with rapidly and slowly inactivating $I_{Ca,}$ respectively) of the I_{Ca} suppression by low pH, with or without ISO. Panel E plots the average of the change on the I_{Ca} values respect to the control condition enhanced by ISO and reduced by low pH in both cell types. Panel F depicts a scatter-gram of suppression of the I_{Ca} (acidosis + ISO) vs. inactivation time constant (τi) for cells with rapidly (●) and slowly (○) inactivating I_{Ca}.

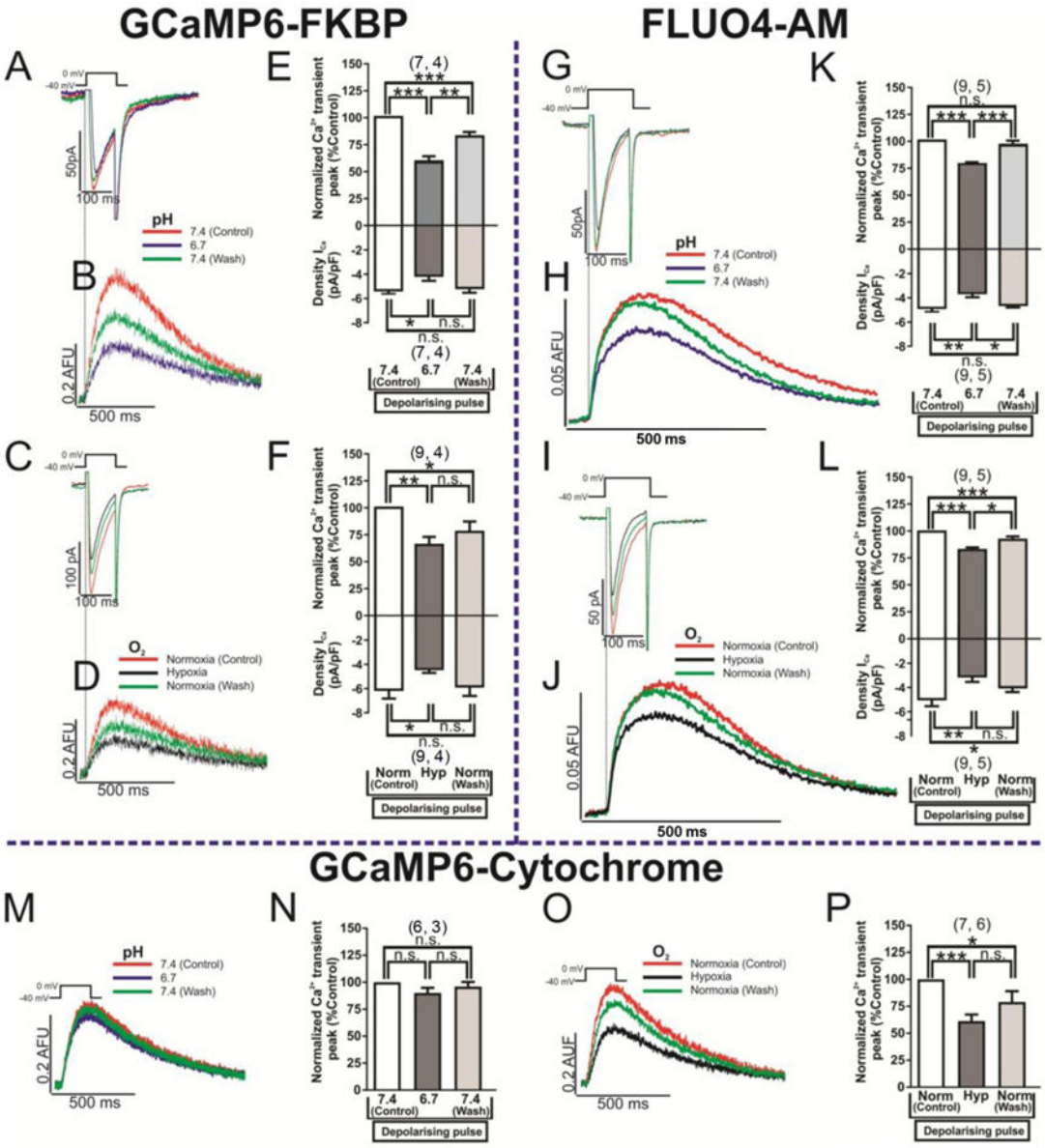

Fig. 8. Global cytosolic calcium, Ca^{2+} microdomains of ryanodine receptors and mitochondria calcium concentration ($[Ca^{2+}]_m$) are affected differentially by hypoxia or acidosis

Panels A and B show original traces of I_{Ca} and focus Ca^{2+} microdomains of RyR2, evoked by voltage-clamp depolarizations and measured with GCaMP6-FKBP probe. The blue records represent the blockade effect of I_{Ca} and Ca^{2+} transients by acidosis (pH=6.7) with respect to the red ones (control, pH=7.4). Panels C and D show original records of I_{Ca} and focus Ca^{2+} microdomains of RyR2 respectively, subjected in this case to treatment with hypoxia (black traces). Panels E and F plots the effects of acidosis and hypoxia, respectively, on the normalized blockade of the Ca^{2+} transient peak (top bars) and density of I_{Ca} (lower bars). Panels G/H (acidosis treatment) and I/J (hypoxia) show original traces of I_{Ca} and global cytosolic Ca^{2+} transients evoked by voltage-clamp depolarizations and measured with the fluorescent dye Fluo4-AM. The red records represent the control condition (pH=7.4 or normoxia), blue traces show low pH signals, black records the treatment with hypoxia and

green traces the wash/out of both stimulus. Panels K and L plot the normalized blockade – by acidosis and hypoxia, respectively – of the Ca^{2+} transient peak (top bars) and density of I_{Ca} (lower bars). Panels M (acidosis treatment) and O (hypoxia) show original traces of mitochondrial matrix Ca^{2+} oscillations evoked by voltage-clamp depolarizations and measured with the cytochrome targeted probe mito-GCaMP6. The red traces represent the control condition (pH=7.4 or normoxia), blue traces show low pH signals, black records the treatment with hypoxia, and green traces the wash/out of both stimulus. Panels N and P plotted the normalized blockade – by acidosis and hypoxia, respectively – of the Ca^{2+} transient peak (top bars) and density of I_{Ca} (lower bars). The duration of the different treatments (pH 6.7 or hypoxia) was 100s.

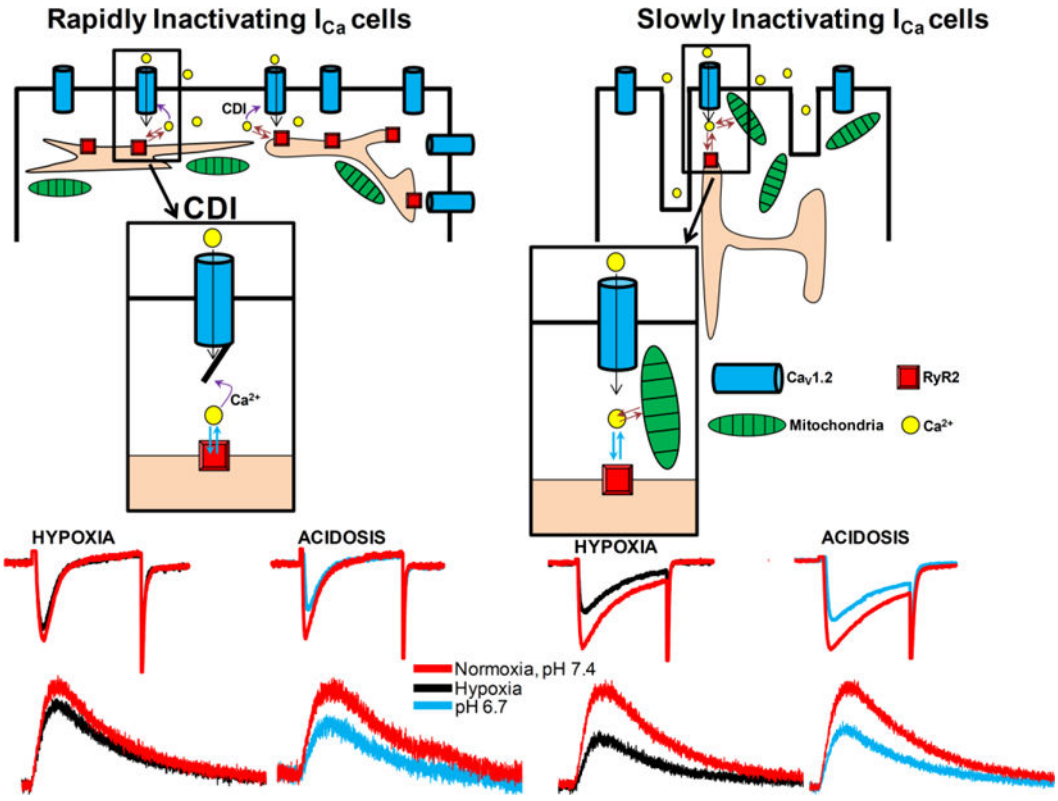

Schematic 1. Ca^{2+} handling by rat neonatal cardiomyocytes during acute hypoxia and acidosis

We found two cell-type populations of rN-CMs during its development in culture with different kinetics of inactivation of the L-type I_{Ca}: rN-CMs with rapidly inactivating I_{Ca} (panel A) predominate during the first days in culture and slowly inactivating I_{Ca} cells (panel A) are more abundant after a week in culture. Acute hypoxia suppresses I_{Ca} more effectively (~40%, panel E) in slowly inactivating I_{Ca} cells compared to rapidly inactivating I_{Ca} cells (~15–20 %, panel C). Suppressive effect of acute acidosis on I_{Ca} (~30–40%, pH 6.7) was not cell-type dependent (panel D and F). Focal RyR2 Ca^{2+} microdomains were suppressed in a similar range as expected from I_{Ca} blockade. Acute hypoxia suppresses I_{Ca} in rapidly inactivating cell population by a mechanism involving Ca^{2+}-dependent inactivation, CDI, insert of panel A, while mitochondrial Ca^{2+} uptake contribute to I_{Ca} suppression in *slowly inactivating* cell population (insert in panel B).

Table 1

Blockade degree (% Control) of the I_{Ca} and different calcium measurements

(global and focal cytosolic Ca^{2+} transients ($[Ca^{2+}]_T$) measured using Fluo-4 AM for global, GCaMP6-FKBP for the focal RyR2 microdomains, and mito-GCaMP6 targeted to mitochondrial matrix to monitor its Ca^{2+} profiles) between both cell types (rapidly and slowly inactivating I_{Ca} cells) for the two different treatments (acidosis and hypoxia). Rapidly and slowly inactivating I_{Ca} cell plots (columns) were compared for interventions, acidosis and hypoxia (rows), using the nonparametric Mann-Whitney rank sum test. Non-significant differences (n.s.) or significant differences between both cell types (in the columns on the right): Data are means ± SE of the number of cells *n* and number of cultures *N* shown in parentheses.

Treatment	Rapidly		Slowly	
	I_{ca}	$[Ca^{2+}]_T$	I_{Ca}	$[Ca^{2+}]_T$
GCaMP6-FKBP (Focal RyR2 μ-domains)				
Acidosis	26.5 ± 6.1 (4, 4)	36.8 ± 4.8 (4, 4)	28.3 ± 7.5 (3, 3) n.s.	38.5 ± 7.5 (3, 3) n.s.
Hypoxia	15.8 ± 4.7 (4, 4)	26.5 ± 6.3 (4, 4)	34.7± 5.3 (5, 4) *	42.0 ± 9.1 (5, 4) n.s.
Fluo-4 AM (Global cytosolic calcium transients)				
Acidosis	32.5 ± 7.2 (5, 4)	22.8 ± 1.6 (5, 4)	31.8 ± 8.1 (4, 4) n.s.	19.6 ± 2.5 (4, 4) n.s.
Hypoxia	23.9 ± 6.7 (5, 4)	17.1 ± 1.7 (5, 4)	42.1± 7.7 (4, 4) *	21.2 ± 3.1 (4, 4) n.s.
GCaMP6-Cytochrome Probe (Mitochondria calcium uptake)				
Acidosis	29.0 ± 5.7 (3, 3)	15.6 ± 5.0 (3, 3)	30.9 ± 6.2 (3, 3) n.s.	5.9 ± 6.2 (3, 3) n.s.
Hypoxia	18.1 ± 4.5 (3, 2)	31.9 ± 4.7 (3, 2)	34.1 ± 3.6 (4, 3) *	41.1 ± 6.6 (4, 3) n.s.

* $P < 0.05$, Mann-Whitney rank-sum test.